Pharm Res (2018) 35:112
https://doi.org/10.1007/s11095-018-2393-6

RESEARCH PAPER

Effect of Chemical Binding of Doxorubicin Hydrochloride to Gold Nanoparticles, *Versus* Electrostatic Adsorption, on the *In Vitro* Drug Release and Cytotoxicity to Breast Cancer Cells

Gamal M. Zayed[1,2] • Islam Kamal[3] • Wael A. Abdelhafez[1] • Fahd M. Alsharif[1] • Mohamed A. Amin[4] • Montaser Sh. A. Shaykoon[5] • Hatem A. Sarhan[6] • Ahmed M. Abdelsalam[1]

Received: 7 December 2017 / Accepted: 19 March 2018

ABSTRACT

Purpose The selective delivery of chemotherapeutic agent to the affected area is mainly dependent on the mode of drug loading within the delivery system. This study aims to compare the physical method to the chemical method on the efficiency of loading DOX.HCl to GNPs and the specific release of the loaded drug at certain tissue.

Method Bifunctional polyethylene glycol with two different functionalities, the alkanethiol and the carboxyl group terminals, was synthesized. Then, DOX·HCl was covalently linked via hydrazone bond, a pH sensitive bond, to the carboxyl functional group and the produced polymer was used to prepare drug functionalized nanoparticles. Another group of GNPs was coated with carboxyl containing polymer; loading the drug into this system by the means of electrostatic adsorption. Finally, the prepared system were characterized with respect to size, shape and drug release in acetate buffer pH 5 and PBS pH 7.4 Also, the effect of DOX.HCl loaded systems on cell viability was assessed using MCF-7 breast cancer cell line.

Results The prepared nanoparticles were spherical in shape, small in size and monodisperse. The release rate of the chemically bound drug in the acidic pH was higher than the electrostatically adsorbed one. Moreover, both systems show little release at pH 7.4. Finally, cytotoxicity profiles against human breast adenocarcinoma cell line (MCF-7) exhibited greater cytotoxicity of the chemically bound drug over the electrostatically adsorbed one.

Conclusion Chemical binding of DOX·HCl to the carboxyl group of PEG coating GNPs selectively delivers high amount of drug to tumour-affected tissue which leads to reducing the unwanted effects of the drug in the non-affected ones.

KEY WORDS bifunctionalized PEG · doxorubicin HCl · electrostatic adsorption · GNPs · MCF-7 · pH sensitive release

ABBREVIATIONS

AIBN	Azobisisobutronitrile
ANOVA	Analysis of variance
DCM	Dichloromethane
DOX·HCl	Doxorubicin HCl
DMSO	Dimethyl sulfoxide
EPR	Enhanced permeability and retention
GNPs	Gold nanoparticles
$HAuCl_4.3\ H_3O$	Hydrogen tetrachloroauric acid trihydrate
IC_{50}	The concentration of substance required for 50% growth inhibition
MCF-7	Breast cancer cell line
MDR	Multi-drug resistance
MWCO	Molecular weight cut off
PCS	Photon correlation spectroscopy
PDI	Polydispersity index
P-gp	P-glycoprotein
PBS	Phosphate buffered saline

Electronic supplementary material The online version of this article (https://doi.org/10.1007/s11095-018-2393-6) contains supplementary material, which is available to authorized users.

✉ Gamal M. Zayed
gamalzayed@hotmail.com

[1] Department of Pharmaceutics and Industrial Pharmacy, Faculty of Pharmacy, Al-Azhar University, Assiut, Egypt

[2] Al-Azhar Centre of Nanosceinecs and Applications (ACNA), Assiut, Egypt

[3] Department of Pharmaceutics and Industrial Pharmacy, Faculty of Pharmacy, Port Said University, Port Fouad, Egypt

[4] Department of Pharmaceutics, Qassim University, Qassim, Kingdom of Saudi Arabia

[5] Department of Pharmaceutical Chemistry, Al-Azhar University, Assiut, Egypt

[6] Department of Pharmaceutics, Faculty of Pharmacy, Minia University, Minia, Egypt

Published online: 30 March 2018

PEG	Polyethylene glycol
RES	Reticulo-endothelial system
SPR	Surface plasmon resonance
TEM	Transmission electron microscope

INTRODUCTION

Nanomedicine-based delivery of chemotherapeutic agents can markedly improve the accumulation of chemotherapeutic agents in the tumor sites as a result of: the enhanced permeation and retention phenomenon (EPR) and lowering the accumulation of the nanocarriers into healthy tissues. In addition, the uptake of chemotherapeutic agents into cancer cells can be adversely influenced when the chemotherapeutic molecule is a substrate to multi-drug resistance (MDR) efflux transporter (e.g. P-glycoprotein, P-gp) as in the case of doxorubicin (1). Nanocarriers are not substrates to MDR transporters and can be endocytosed into the cancer cells. Although earlier release of the chemotherapeutic agent into the cytoplasm might be exposed to P-gp, nanocarriers that only disassemble or release their cargo following endosomal uptake have better chance to evade P-gp-mediated efflux (2). In this regard, pH-dependent drug release can help to avoid the immature drug release in the blood circulation (pH 7.4) and can only take place at the tumor microenvironment (pH 3–6). Furthermore, the ones that are taken up into the cancer cells can further release drug load into the acidic environment of the endosomal-lysosomal system (pH 5) (3).

GNPs are regarded as useful, safe and biocompatible in the field of targeted drug delivery (4–6). Coating of GNPs with hydrophilic PEG corona dramatically enhances both the *in vitro* as well as the *in vivo* stability due to steric stabilization rather than electrostatic one (7) . Uncoated GNPs are likely to be accumulated in liver and spleen (reticuloendothelial system) due to the hydrophobic nature and the absence of the hydrophilic coat provided by PEG molecules. Alternatively, PEGylated GNPs have minimum affinity to adsorb plasma protein and consequently can evade uptake by RES. This results in long blood circulation time giving them the chance for tumor extravasation and to act as an excellent sustained drug delivery approach (7,8). Based on these facts, PEGylated GNPs could be taken by cancer cells more efficiently than non-PEGylated ones (9,10).

Doxorubicin hydrochloride (DOX·HCl) is a well-known chemotherapeutic agent with a broad-spectrum activity against several types of cancer. This drug is regarded as one of the most potent approved chemotherapeutic agents (11). The drug acts by binding to DNA-associated enzymes, intercalating with DNA base pairs, and targeting multiple molecular targets to produce a range of cytotoxic effects that results in cancer cell apoptosis (12).

The loading of the cytotoxic agent to the nanomaterial along with strategy of its targeting are highly important factors for targeted and selective drug therapy. The drug may be physically adsorbed, covalently attached to the nanomaterial surface or it can be encapsulated into particle core as in case of polymer based-nanoparticles. It has been reported that covalent linking is likely to be more advantageous than other ways of attachment and loading as it enables better control over the number of drug molecules attached to the nanomaterial. Also it provides a more precise control of the amount of therapeutic compound delivered to specific sites (13).

Steric stabilization by surface PEGylation of nanoparticles is very important because it prolongs circulation time, prevents nanoparticles aggregation, minimizes phagocytosis and shields form opsonization. Chemical binding of DOX·HCl to PEG coated GNPs by covalent pH sensitive bond will result in smart nanocarriers system for effective and selective cancer treatment. In such system, GNPs will have more than one function. Firstly, the PEG corona of GNPs will act as a platform to which the chemotherapeutic agent can be attached by acidic sensitive bond. This acidic sensitive bond cleaves at the acidic pH of tumor tissues (5,14–19). Secondly, the functionalized nanoparticles will be accumulated in the tumor tissue by EPR effect leading to decrease of the required drug dose and side effects (20). Additionally, GNPs produce heat upon exposure to laser leading to physical treatment of the tumor via the thermal ablation (21). The whole designed system can combine physical treatment, due to GNPs, with chemotherapeutic one, due to the attached drug, as a new approach for cancer therapy.

The main aim of the present work is to selectively deliver DOX·HCl to the diseased parts inside the body for efficient cancer treatment. Hence, a comparative study between two different DOX·HCl loaded GNPs systems was established. The first system was based on the chemical binding of DOX·HCl to the surface of GNPs through PEG-undecanethiol spacer by a pH sensitive hydrazone bond. The second system was based on the non-covalent binding of DOX·HCl to the carboxy-functionalized GNPs via an electrostatic attraction. Moreover, the two systems were subject to an *in vitro* drug release study followed by the evaluation of their cytotoxic activity against breast cancer cell line (MCF-7).

EXPERMENTAL

Materials

Hydrogen tetrachloroaurate (III) trihydriate ($HAuCl_4.3H_2O$) and thioglycolic acid were purchased from Acros organics, Belgium. Trisodium citrate dihydrate was supplied by fisher

scientific company, USA. Polyethylene glycol 2000 g/mol and ellman's reagent were purchased from alfa aeser, Germany. Doxorubicin hydrochloride was provided by Beijing mesochem technology company, Beijing, China. *P*-toluene sulphonyl chloride was purchased from lobachemi, India. AIBN (azobisisobuteronitrile), hydrazine hydrate, thionyl chloride and silver oxide were purchased from Sigma Aldrich, Germany. Potassium iodide and anhydrous sodium sulphate were supplied from El-Nasr pharmaceutical chemical Company, Egypt. Thioacetic acid was purchased from Tokyo chemical industries (TCI), Japan. 11-bromoundecene was purchased from Waco pharmaceutical company, Japan. Dialysis tubing (MWCO 12–14 kd) was provided by Serva electronics GmbH, Heidelberg, Germany. All the solvents were dried over molecular sieve 4–8 mesh before use.

Synthesis of carboxy-PEG-undecane Thiol and doxorubicin-PEG-undecanethiol Conjugate

Synthesis of monotosyl-PEG (1)

Compound 1 was synthesized by dissolving PEG (2000 g/mol, 10.0 g, 5.0 mmol) in dry DCM (500 ml), the resulting clear solution was chilled to 0°C in an ice bath under nitrogen atmosphere. Then silver oxide (1.738 g, 7.50 mmol, 1.5 eq.) and potassium iodide (0.332 g, 2.0 mmol, 0.4 eq.) were added to the solution under stirring. *p*-toluene sulfonyl chloride (1.0 g, 5.25 mmol, 1.05 eq.) was dissolved in sufficient volume of dry DCM and quickly added to the rapidly stirred reaction mixture. Reaction was left under nitrogen for 2–4 h, during this period the reaction progress was TLC monitored till completion. Reaction mixture was then filtered to remove inorganic salts, washed with water, dried over anhydrous sodium sulphate, concentrated to small volume by rotary evaporator, precipitated by dropping into ice-cooled diethyl ether, separated by filtration and, finally, dried under vacuum. (yield 8.5 g, 78.9%).

^{1}H-NMR (400 MHz, DMSO-d_6, δ ppm): 7.78 (2H, d, J = 8.0, aromatic C**H**), 7.48 (2H, d, J = 8.0, aromatic C**H**), 4.47 (1H, s, PEG-O**H**), 4.14 (2H, t, -$CH_2C\mathbf{H_2}$-OH), 3.70 (2H, t, $CH_2C\mathbf{H_2}OTs$), 3.60–3.50(m, PEG backbone), 3.35(2H, t, $C\mathbf{H}_2CH_2OTs$),, 2.44 (3H, s, $C\mathbf{H}_3$).

Synthesis of Polyethylene Glycol Ethyl Thioacetate (2)

Under nitrogen atmosphere, compound 1 (5.0 g, 2.4 mmol) was dissolved in dry ethanol (60 ml) with gentle heating, followed by drop wise addition of sodium hydroxide (0.479 g, 12.0 mmol, 5 eq.) and thioglycolic acid (10 g, 12.0 mmol, 5 eq.). The reaction was refluxed under nitrogen for 48 h. Then, the mixture was cooled to room temperature, quenched with dilute hydrochloric acid and the solvent was evaporated to dryness under vacuum. Residue was dissolved in dichloromethane (20 ml), washed twice with water, dried over anhydrous sodium sulphate, reduced to small volume and precipitated by dropping into ice cooled diethyl ether. The product was separated by filtration, washed with cold ether and dried, (yield 3.9 g, 81%).

^{1}H-NMR (400 MHz, $CDCl_3$, δ ppm): 3.97(1H, s, $CH_2O\mathbf{H}$), 3.83 (2H, t, J, 4.0 Hz, $C\mathbf{H}_2CH_2SCH_2$), 3.73 (2H, t, J = 4.0 Hz, $C\mathbf{H}_2OH$), 3.60–3.50 (m, PEG backbone), 3.48 (2H, s, $CH_2SC\mathbf{H}_2COOH$), 2.91 (2H, t, J, 4.0 Hz, $CH_2C\mathbf{H}_2SCH_2$).

Synthesis of S-(11-bromoundecyl) Thioacetate (3)

Under nitrogen atmosphere, 11-bromoundecene (4.00 g, 3.77 ml, 17.15 mmol) was mixed with dry toluene (250 ml), followed by addition of thioacetic acid (7.43 g, 97.7 mmol, 5.7 eq.). Then, AIBN (0.8 g, 4.8 mmol 0.28 eq.) was added and reaction mixture refluxed under nitrogen for 3 h. The reaction was cooled down to room temperature and washed several times with saturated sodium bicarbonate solution (3 × 200 ml) when the organic phase was separated and dried over anhydrous magnesium sulfate. Toluene was removed under reduced pressure, crude product was purified by column chromatography using petroleum ether:methylene chloride 4:1 (yield 3.7 g, 69.7%).

^{1}H-NMR (400 MHz, $DMSOd_6$, δ ppm): 3.47 (2H, t, J, 4.0 Hz, $CH_2\mathbf{CH_2}Br$), 2.81 (2H, t, J, 4.0 Hz, $CH_2C\mathbf{H_2}SCOCH_3$) 2.30 (3H, s, $CH_2SCOC\mathbf{H_3}$), 1.80 (2H, t, J, 4.0 Hz, $C\mathbf{H_2}CH_2SCOCH_3$), 1.50 (2H, t, J, 4.0 Hz, $C\mathbf{H_2}CH_2Br$), 1.39–1.26 (14H, m, undocyl backbone).

Synthesis of Carboxy-Polyethylene Glycol Undecanethioacetate (4)

Under nitrogen atmosphere, compound 2 (2074.4 g/mol, 2.0 g, 0.964 mmol) was let to melt in an oil bath with gentle stirring. Then sodium hydroxide pellet (0.385 g, 9.64 mmol, 10 eq.) was added to the melt and the mixture was stirred for an hour. A solution of compound 3 (1.193 g, 3.8 mmol, 4 eq.) in dry acetonitrile (50 ml) was added in and reaction was refluxed for 12 h. Reaction mixture was then cooled to room temperature, neutralized with dilute hydrochloric acid and the solvent was removed under reduced pressure to dryness. Residue was dissolved in dichloromethane, washed with water and dried over anhydrous sodium sulphate and concentrated to small volume. Pure dried product (compound 4) was obtained after precipitating DCM solution into ice cooled diethyl ether, separated by filtration and dried under vacuum (yield 1.4 g. 63%).

^{1}H-NMR (400 MHz, $CDCl_3$) δ ppm, 3.80–3.46 (m, PEG backbone), 3.45 (2H s, $SC\mathbf{H_2}COOH$), 2.85 (2H t, J, 4.0 Hz,

$C\mathbf{H_2}CH_2OCH_2$), 2.67 (2H t, J, 4.0 Hz, $CH_2C\mathbf{H_2}SCOCH_3$), 2.49 (2H t, J, 4.0 Hz, $CH_2C\mathbf{H_2}SCH_2COOH$), 2.31 (3H s, $C\mathbf{H_3}COSCH_2$), 1.81–1.26 (22H m, alkyl chain).

Synthesis of Carboxy-Polyethylene Glycol Undecane Thiol (5)

Methanolic HCl (11.6 ml of 2 M) was added to 0.5 g (2302.8 g/mol, 0.217 mmol) of compound 4 dissolved in 5 ml of dry methanol. The reaction mixture was refluxed overnight, solvent removed under reduced pressure to afford the residue of the free thiol. Residue was dissolved in 10 ml of DCM, precipitated by dropping in ice cooled diethyl ether, filtered and dried under reduced pressure (yield 400 mg, 80.4%). Formation of free thiol of compound 5 was confirmed by testing with Ellman's reagent (prepared in 0.1 M phosphate buffer pH 8 in presence of 1 mM EDTA). The prepared sample was incubated with 50 µl of the reagent solution for 15 min in the dark at 37°C and the obtained yellow color was measured at 412 nm using UV-Vis spectroscopy indicating a positive free thiol.

^{1}H-NMR (400 MHz, $DMSOd_6$, δ ppm): 3.69 (2H t, J, 4.0 Hz, $C\mathbf{H_2}CH_2S$), 3.60–3.51 (m, PEG backbone), 3.41 (2H s, $SC\mathbf{H_2}COOH$), 2.82 (2H, bs, $C\mathbf{H_2}CH_2OCH_2$), 2.74 (2H t, J, 4.0 Hz, $CH_2C\mathbf{H_2}SCOCH_3$), 2.68 (2H t, J, 4.0 Hz, $CH_2C\mathbf{H_2}SCH_2COOH$), 1.62 (2H t, J, 4.0 Hz, $C\mathbf{H_2}CH_2SCOCH_3$), 1.51(2H t, J, 4.0 Hz, $C\mathbf{H_2}CH_2OCH_2$), 1.24 (14H bs, alkyl chain), 0.86 (1H t, J, 4.0 Hz, CH_2-S**H**).

Synthesis of Undecanethiol- Polyethylene Glycol Hydrazide (5')

To a solution of compound 4 (1.0 g, 0.434 mmol) in dry DCM (30 ml), thionyl chloride (0.258 g, 2.17 mmol, 5 eq.) was added drop wise in an ice bath. Reaction was vigorously stirred at 4°C for 4 h then at room temperature for 6 h, followed by removal of DCM and excess thionyl chloride by distillation. The acid chloride residue was re-dissolved immediately in DCM (20 ml) and treated with hydrazine monohydrate (0.065 g, 1.30 mmol, 3 eq.) and a drop of triethylamine in an ice-bath and the reaction was left under stirring at room temperature for 6 h. The reaction mixture was filtered, evaporated to dryness. The residue was dissolved in DCM and dropped into ice cooled diethyl ether an the solid product was separated by filtration and dried under vacuum. (yield 0.7 g, 70%).

^{1}H-NMR (400 MHz, $DMSOd_6$, δ ppm); 8.16 (1H s, CO-N**H**-NH_2), 3.71 (2H s, CO-NH-N$\mathbf{H_2}$) 3.68–3.50 (m, PEG backbone), 3.41 (2H s, S-C$\mathbf{H_2}$-CO), 2.90 (2H t, J, 4.0 Hz, $C\mathbf{H_2}CH_2OCH_2$), 2.78 (2H t, J, 4.0 Hz, $CH_2C\mathbf{H_2}SCOCH_3$), 2.68 (2H t, J, 4.0 Hz, CH2C$\mathbf{H_2}SCH_2COOH$), 1.67(2H t, J, 4.0 Hz, $C\mathbf{H_2}CH_2SCOCH_3$), 1.59 (2H t, J, 4.0 Hz, $C\mathbf{H_2}CH_2OCH_2$), 1.23 (14H m, alkyl chain), 1.09 (1H t, J, 4.0 Hz, CH_2-S**H**).

Synthesis of Doxorubicin HCl-Polyethylene Glycol Conjugates through pH-Sensitive Hydrazone Linkage (6')

Under nitrogen atmosphere, DOX·HCl (0.033 g, 0.0571 mmol) was added to 0.162 g of undecane thiol-PEG-hydrazide (0.0571 mmol, 1 eq.) dissolved in 10 ml of dry methanol. Mixture was vigorously stirred under nitrogen for 5 min before addition of glacial acetic acid (0.102 g). The reaction mixture was stirred under nitrogen at room temperature in the dark for 24 h. Reaction progress was monitored by TLC using methanol:chloroform 4:6. (R_f, DOX·HCl 0.3, Dox.-Conj 0.7). Then, methanol was removed by evaporation under vacuum, PEG-DOX conjugate was dissolved in chloroform, filtered to remove unreacted DOX·HCl residue. Chloroform solution was concentrated to small volume by rotary evaporation, precipitated in cold diethyl ether, product separated by filtration and dried under vacuum, yield (98.2 mg, 48.6%).

^{1}H-NMR (400 MHz, $CDCl_3$, δ ppm): the characteristic DOX peaks obtained at 7.97, 7.71, 7.45, 1.99, 1.89, 1.13, 1.12 and 0.79 ppm. 7.97(H bs), 7.71 (H bs), 7.45 (H, bs) 3.72–3.42 (m, PEG backbone), 2.98–2.61 (m, alkyl chain), 1.99–0.75 (m, aliphatic peaks of DOX).

Preparation of Citrate Stabilized Gold Nanoparticles

GNPs were synthesized according to the method described in the literature (22), Briefly, hydrogen tetrachloroaurate was brought to boiling and reduced by the rapid addition of sodium citrate. An optimized gold/citrate ratio was prepared as follows, in 100 ml rounded bottom flask 97 ml of distilled water and 1 ml of 1% $HAuCl_4.3H_2O$ was heated under reflux until boiling, and then 2 ml aqueous solution of tri-sodium citrate dihydrate solution was added to the flask rapidly. Boiling and stirring continued for 15 min. After that, the heating was ceased and the solution was stirred until it was cooled down to room temperature. Stock solutions of the gold salt (10 mg/ml, 1%) and trisodium citrate (100 mg/ml, 10%) were prepared using deionized water and were filtered through 0.22 µm membrane filter.

Loading of Doxorubicin Hydrochloride Via the Self-Assembly of DOX-PEG Undecanethiol Conjugate to the Surface of Citrate Stabilized GNPs

The preparation of DOX·HCl loaded GNPs was based on the self-assembly of the DOX-PEG-undecanthiol over the surface of GNPs to obtain GNPs functionalized with the exposed DOX·HCl on their surface. Briefly, 29.42 mg of the DOX-PEG-undecanthiol conjugate (contains 17% weight DOX·HCl) was added to 25 ml of citrated capped GNPs colloidal dispersion in order to obtain a final concentration of 1.1768 mg/ml of the DOX-PEG conjugate (equivalent to

200 μg/ml free DOX·HCl). The mixture was stirred for 24 h in the dark, dialyzed against distilled water for 24 h to remove unbound DOX.HCl and DOX-polymer conjugate. However, the prepared GNPs-PEG-DOX assembly was characterized for their size and zeta potential. In addition, the amount of unbound DOX-PEG conjugate was determined spectrphotomertically at 480 nm (23). Also, the percentage amount of loaded drug was calculated using the following equation:

$$\%of\ \ loaded\ DOX = \frac{total\ DOX-PEG\ conj}{dialysed\ DOX-PEG\ conj} x\ 100 \qquad (1)$$

Where *total DOX-PEG conj*: the total weight of DOX-PEG conjugate added and *dialyzed DOX-PEG conj* represents the amount of the unbound DOX and DOX-PEG in the dialysate (23).

Preparation of Carboxyl Functionalized Gold Nanoparticles and Adsorption of Doxorubicin Hydrochloride

To prepare GNPs-loaded with doxorubicin hydrochloride loaded via electrostatic adsorption strategy, GNPs were first functionalized with the previously synthesized carboxyl PEG-undecanthiol (compound 5). In a typical procedure, excess amount (50 mg) of the modified PEG was added to 25 ml of the citrate stabilized GNPs and left stirring for 24 h. The thiol end group of the polymer was adsorbed on the gold replacing most of the adsorbed citrate anions on the particle surface with the carboxy modified PEG. Then, 5 mg of DOX·HCl was added and left under stirring in the dark for additional 12 h to saturate the polymer carboxyl terminal with the positively charged doxorubicin hydrochloride. However, the mixture was dialyzed for 24 h in dialysis tubing to remove unbound drug and polymer, and the percentage amount of adsorbed DOX·HCl was calculated from the following equation:

$$\%\ \ of\ \ loded\ DOX.HCl = \frac{A-B}{A}\ x\ 100 \qquad (2)$$

Where *A*: the total amount of DOX·HCl added and *B*: the amount of the unbound DOX·HCl in the dialysate. The free unbound DOX·HCl in the dialysate was determined by UV- vis spectroscopy at 480 nm.

IR and ^{1}H-NMR Spectroscopy

The FT-IR analysis was carried out using "Nicolet 6700 FT-IR instrument, Thermo-Fischer scientific corporation, USA. The ^{1}HNMR analysis was carried out using "Bruker Avance III 400 MHz for ^{1}H and 100 MHz for ^{13}C (Bruker AG, Switzerland) with BBFO Smart Probe and Bruker 400 AEON Nitrogen-Free Magnet".

Particle Size and Zeta Potential Measurement

The particle size, size distribution and the zeta-potential of the prepared plain GNPs, along with polymer coated GNPs and drug loaded GNPs were analyzed by photon correlation spectroscopy (PCS) using Zetasizer ZSNano 90 (Malvern instruments, UK). Analysis time was 60 s and the zeta potential of nanoparticulate dispersions was determined as such without dilution.

Transmission Electron Microscopy (TEM) Imaging of the Nanoparticles

The morphology of the prepared GNP**s** was determined by TEM imaging. TEM samples were prepared by dropping gold colloids on carbon-coated copper grids and dried at room temperature. The samples were observed on a JEM-100CXII transmission electron microscope (JEOL Ltd, Japan).

Effect of Sodium Chloride and Different Buffers on the Dispersion Stability of the Prepared GNPs

The dispersion stability of both citrate and polymer capped GNPs was investigated in different conditions including PBS (pH 7.4), acetate buffer (pH 5) and at high ionic strength (5 M sodium chloride solution) as well. Briefly, known volumes of both citrate and polymer capped colloidal gold dispersions were treated with 200 μl/ml of the colloidal dispersion of both PBS pH 7.4 and acetate buffer pH 5 and with 150 μl per milliliter of colloidal dispersion of 5 M sodium chloride solution. The dispersion stability of different nanoparticle preparations was monitored by changes in UV-Vis absorbance, size and zeta potential.

In Vitro Release Study of the Prepared DOX·HCl Loaded GNPs

The release behavior of the drug from different GNPs preparations was assessed in two different buffer systems, the PBS (pH 7.4) and the acetate buffer (pH 5) to simulate the physiological pH of blood circulation and mimic cancer acidic environment, respectively. The release behavior of the drug from both formulae was compared with the release behavior of pure drug to figure out the effect of different loading strategies of GNPs on the drug release profiles. DOX·HCl release from the investigated systems was monitored over the period of 72 h. 3 ml of each system, pure drug, chemical bound drug and adsorbed one, were sealed in dialysis membrane tubing (MWCO 12–14 KD) and immersed in 50 ml of the release buffer at 37°C and shaked at 50 rpm in a shaking water bath. 3 ml of the release medium was withdrawn at different time intervals and replaced with equal volumes of fresh buffer to keep the volume of the release medium constant. The amounts of DOX·HCl released were determined using UV-Vis spectroscopy at 480 nm.

In Vitro Cell Viability Assay of Doxorubicin Loaded GNPs against MCF-7 Breast Cancer Cell Line

MTT assay of the designed systems was assessed against MCF-7 breast cancer cell line. The human breast adenocarcinoma (MCF-7) cells were obtained from Vacsera, Egypt. Cells were routinely grown with RPMI-1640 medium containing 10% fetal bovine serum (Sigma-Aldrich, Germany). Cells were grown at 37°C in 25 ml flasks (purchased from Thermo Fisher scientific, USA) in a humidified atmosphere containing 5% CO_2. Cells were generally replicated once a week, and culture medium was renewed once or twice between two replications; 10,000 MCF-7 cells were seeded in each well of 96-well plates. 24 h later, cells were treated with free DOX·HCl, chemically linked DOX·HCl-GNPs and physically adsorbed DOX·HCl-GNPs for 48 h. At the end of the incubations, the medium was removed, cells were washed with buffered saline. The number of surviving cells was estimated using 3-(4,5-dimethylthiazol-2-yl)-2,5-diphenyl tetrazolium bromide (MTT) assay (BIO BASIC CANADA INC). Briefly, after removing the medium, MTT reagent (200 µL diluted in culture medium, 0.5 mg/ml) was added. After 4 h incubation, the MTT/medium was removed, and DMSO (200 µL) was added to dissolve the formazan crystals. The absorbance of the colored solution was measured on a microplate reader at λ_{max} 525 nm and λ_{max} 620 nm. Results were evaluated by comparing the absorbance of the treated cells with the absorbance of wells containing cells treated with solvent alone. Conventionally, cell viability was estimated to be 100% in the control. All experiments were performed in triplicate. The concentration of substance required for 50% growth inhibition (IC_{50}) was estimated as that giving a 50% decrease in absorbance relative to control. The obtained viability results were statistically analyzed using the non-parametric "Kruskal-Wallis test" through a graph pad-prism software program.

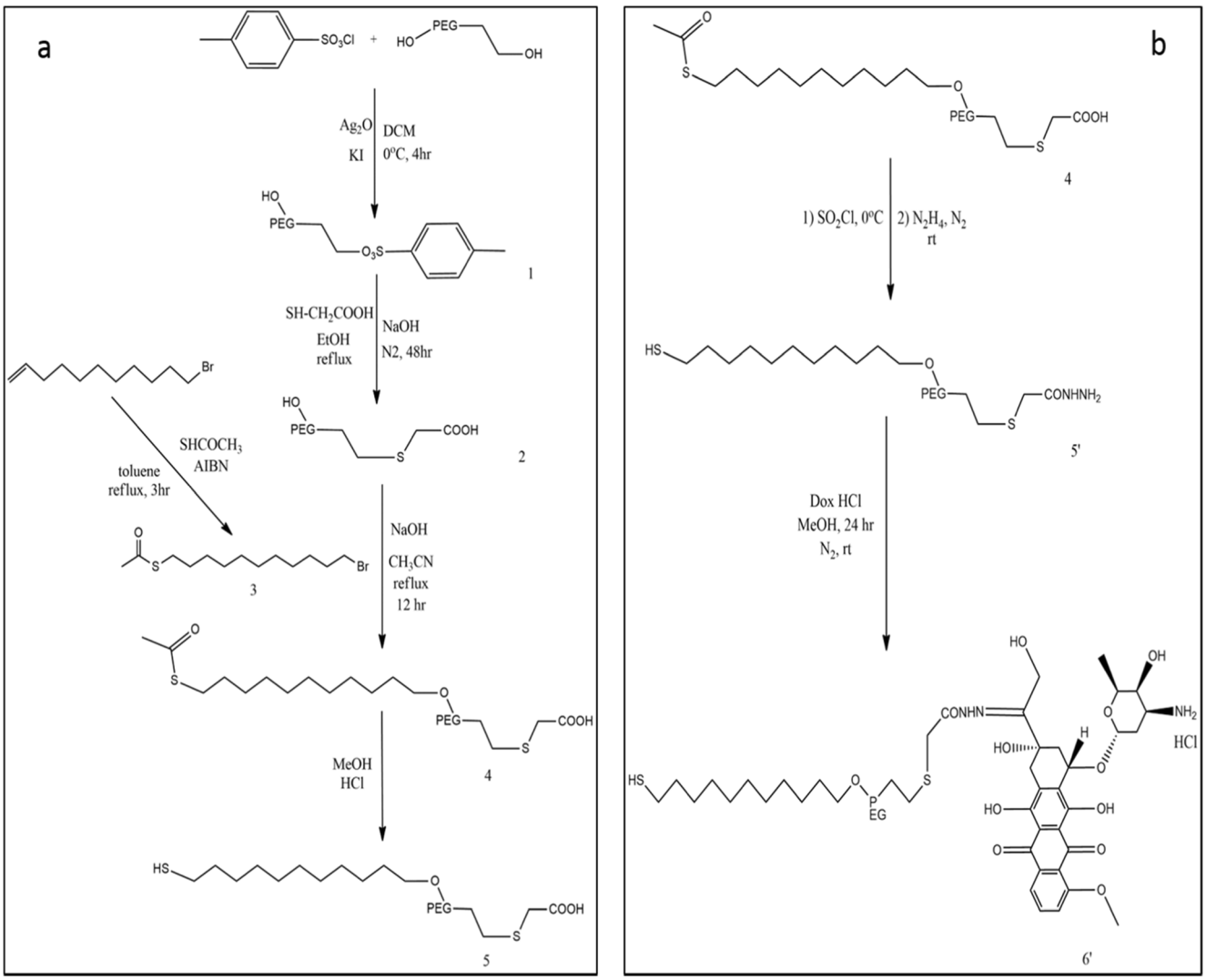

Scheme 1 Synthesis of carboxy-PEG undecanethiol (**a**) and synthesis of Dox-PEG-undecane thiol conjugate (**b**).

RESULTS AND DISCUSSION

Synthesis of carboxy-PEG-undecane Thiol and the DOX-PEG-Undecane Thiol Conjugate

Synthesis of the Carboxy-PEG-Undecane Thiol

The synthesis of monotosyl-PEG was adopted according to method described in the literature (24–27). Monotosylation was achieved in a high yield by treating of PEG diol with silver oxide, where silver cation coordinates with PEG. Then, the addition of one equivalent of p-toluene sulphonyl chloride resulted in the formation of monotosylation. The formation and the purity of monotosylate were confirmed by ^{1}H-NMR. The previous step was followed by synthesis of PEG-ethyl thioacetate which was prepared by reaction of monotosylate with thioacetic acid in presence of base as previously reported with slight modifications (28,29). The monotosylated product was subjected to a nucleophilic substitution reaction using thioglycolic acid and sodium hydroxide in absolute ethyl alcohol (Scheme 1a). A similar reaction was patented by Bogdanov *et al.* using dioxan in presence of 4-dimethylaminopyridine (29). The produced PEG was carboxyl functionalized through a thioether bridge as can be seen in Scheme 1a.

On the other hand, the conversion of the bromoundecene into a bromoundecylthioacetate was described by *Moldt and coworkers* (30), where an anti-markovnikov addition reaction of thioacetic acid to the terminal double bond of bromodecene was catalyzed by AIBN, a radical initiator that was described in several literature work (31–33). Followed to that was, the synthesis of carboxy-PEG-undecane thioacetate according to Williamson reaction of the free hydroxyl terminal of the polyethylene glycol ethyl thioacetate with the thiol protected bromoundecane in the presence of excess of either sodium or potassium hydroxide (Scheme 1a) (33–35).

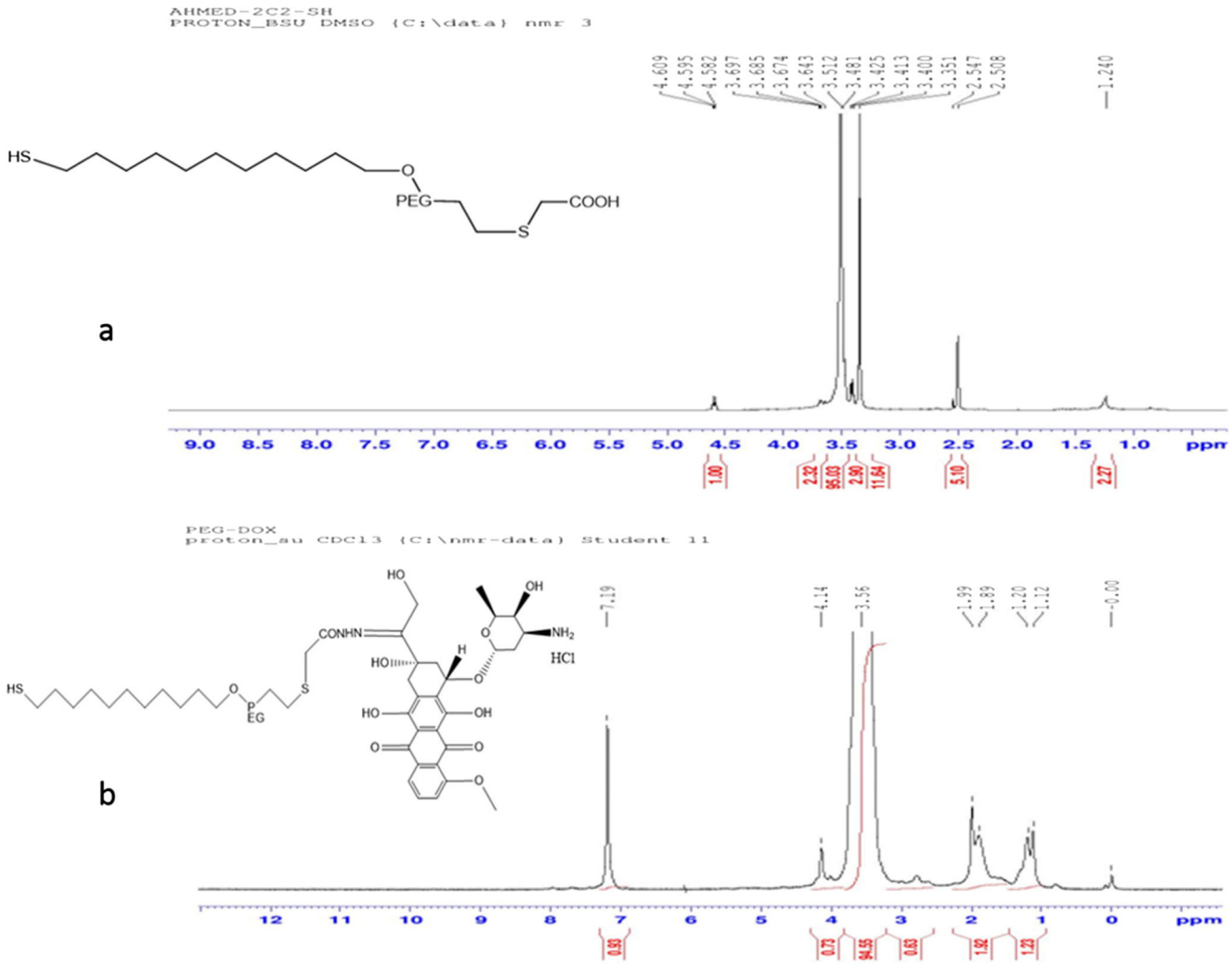

Fig. 1 ^{1}H-NMR spectrum of carboxy-PEG-undecane thiol (**a**) and Dox-PEG undecane thiol (**b**).

Table 1 Size, Zeta Potential, PDI and % Drug Loading Values for the Developed GNPs-Dox HCl Systems Compared to the Unloaded GNPs

	Citrate capped GNPs	Chemically bound GNPS-Dox	Physically adsorbed GNPs-Dox
Size (nm)	36.47 ± 0.22	40.37 ± 0.52	40.29 ± 1.45
Zeta potential (mV)	−42.1 ± 0.5	−20 ± 0.2	−27 ± 0.6
PDI	0.3 ± 0.02	0.281 ± 0.09	0.268 ± 0.11
% loaded Dox HCl	–	99%	92%

Synthesis of carboxy-PEG-undecane thiol was based on the liability of thioacetate protecting group to hydrolyze in either acidic or basic conditions (36). However, hydrolysis in acidic medium was applied, where methanolic HCl was generated *in situ* through the reaction of acetyl chloride with dry cooled methanol (37). ^{1}H-NMR spectrum of the produced free thiol compound in DMSO is displayed in Fig. 1a. As can be seen, the complete disappearance of the singlet peak at 2.3 ppm corresponding to thioacetate protection was noticed. Also, the formation of free thiol was confirmed using Elman's reagent (38).

Synthesis of DOX-PEG-undecane Thiol Conjugate

As shown in Scheme 1b, to bind DOX·HCl chemically to the carboxy functionalized PEG molecule, the hydrazide-PEG derivative was first synthesized based on the usual thionyl chloride activation method. The produced acid chloride derivative is highly reactive and was directly treated with excess amount of hydrazine monohydrate to give the desired hydrazide product. On the other hand, the basic conditions provided by the addition of triethylamine and excess hydrazine monohydrate serve for reduction of the conversion of terminal thioacetate into free thiol (36,39). This was followed by conjugating DOX·HCl molecule to the hydrazide-PEG. The synthesis of doxorubicin bound molecules was described in literature (5,40)**.** The employment of hydrazide bond to load this cytotoxic drug onto the PEG molecule was investigated by Wang *et al*... (41) was found to have beneficial properties regarding the behavior of the drug release and the effect against multidrug resistant cancer cell lines. The synthetic strategy was adapted in dry methanol in the presence of catalytic amount of glacial acetic acid; however a similar procedure was described by Etrych *et al* (42). The obtained product was identified by the appearance of the characteristic peaks of DOX·HCl at 1.1, 1.9, 7.4, 7.7 and 7.9 ppm as illustrated in the ^{1}H-NMR spectrum (Fig. 1b).

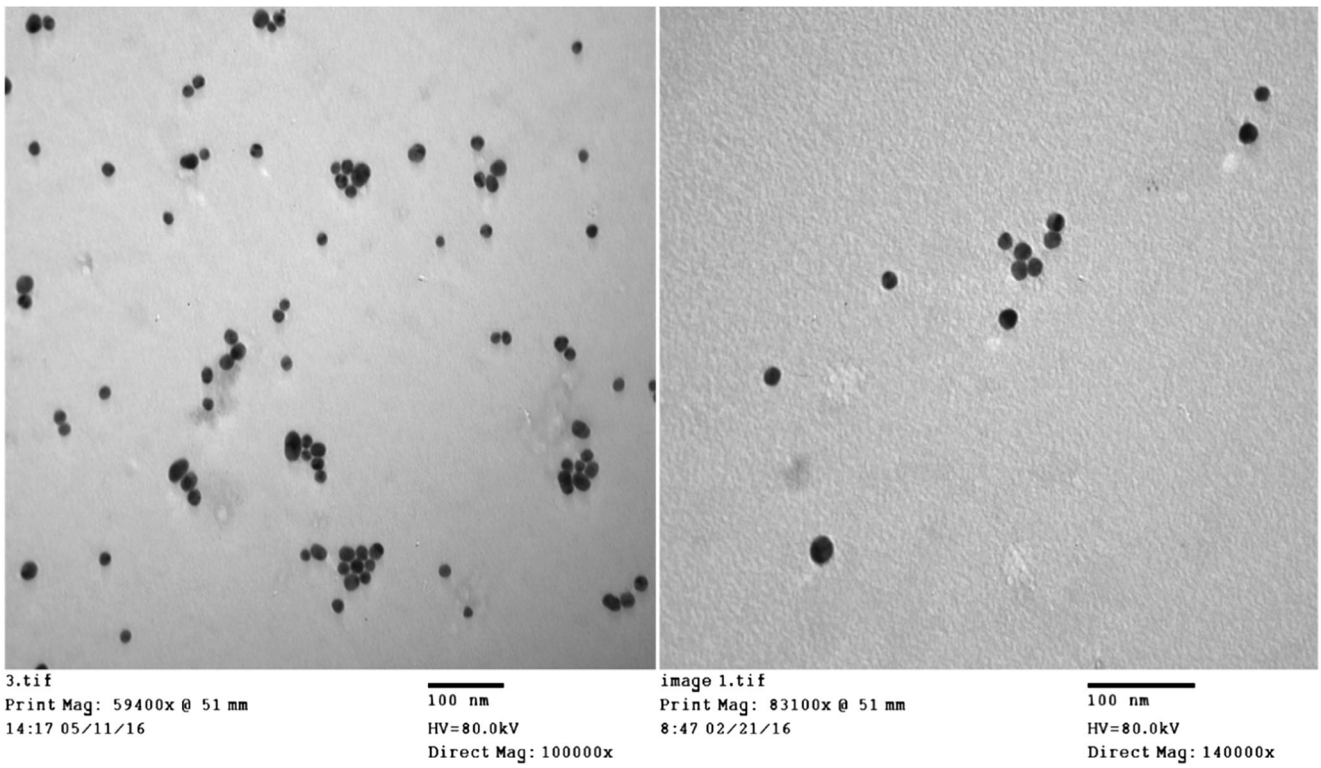

Fig. 2 TEM images of the synthesized GNPs.

Preparation and Characterization of GNPs

Sodium citrate reduction method was applied for preparation of citrate stabilized GNPs as described by *Turkovich* and *Frens* (22,43). The produced GNPs were of average size of 36.47 nm with PDI of 0.3 and zeta potential of −42 mV (Table I). Moreover, TEM images showed that nanoparticles are nearly spherically in shape as depicted in Fig. 2. The size calculated by TEM is smaller than the size determined by PCS because light scattering (PCS) determines the hydrodynamic size of the particles (the particles, adsorbed citrate anions and the surrounding moving layer of water). In contrast, TEM detects only the electron dense mass of the particles without the surrounding layer of water and electrolytes. On the other hand, the UV-Vis spectrum of the prepared GNPs showed a strong absorption band in the visible region with marked SPR maximum at 520 nm.

Preparation and Characterization of DOX·HCl Capped GNPs

The preparation of DOX·HCl functionalized GNPs was followed by two different capping strategies; the electrostatic adsorption and the covalent binding strategies. However, Table I illustrates the size, zeta potential and PDI values of the developed GNPs-DOX systems compared to the citrate capped GNPs. The increase in GNPs size from 36.47 nm (before drug capping) to 40.29 nm and 40.39 nm for physically adsorbed and chemically bound DOX·HCl, respectively, was believed to be an indication for efficient nanoparticles coating with polymer and consequently drug capping to GNPs (44,45). Moreover, successful coating resulted decreasing the negative value of zeta potential value from −42 mV for the uncoated GNPs to −27 mV for the electrostatically adsorbed DOX·HCl and − 20 mV for the chemically bound

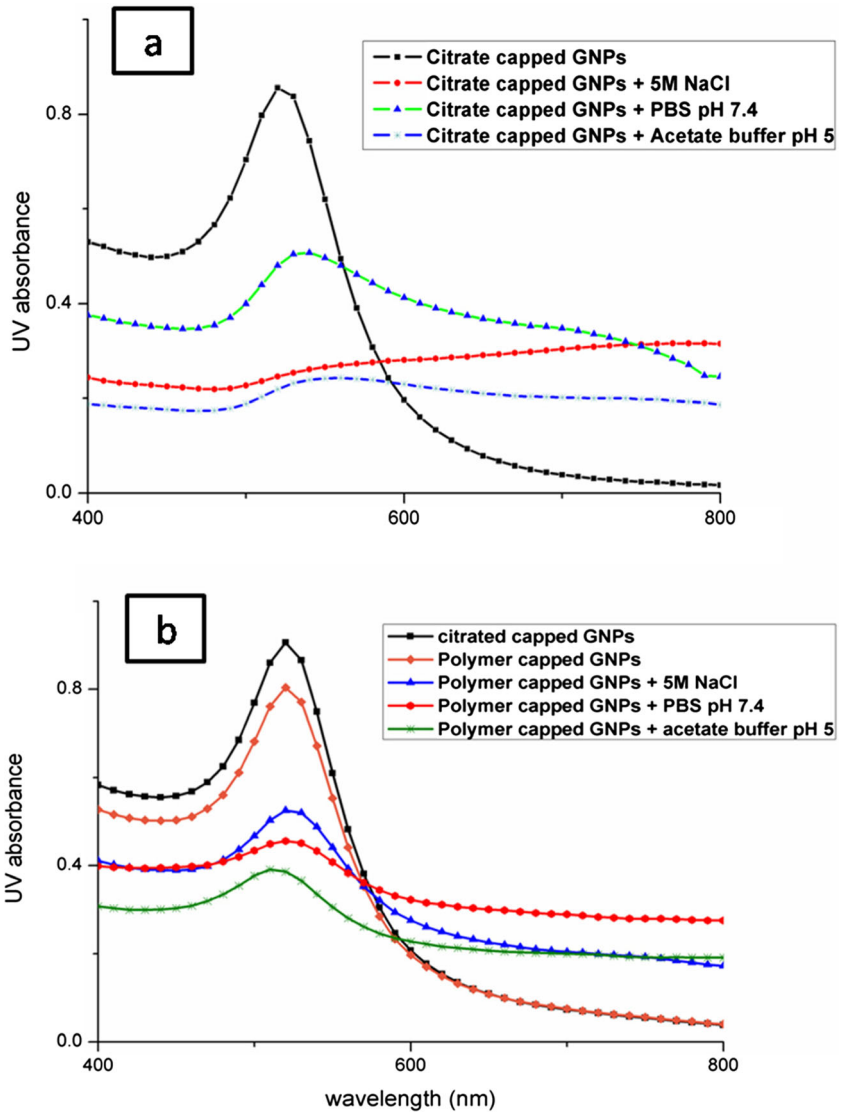

Fig. 3 UV-SPR spectrums of the dispersion stability of citrate capped GNPs (**a**) and polymer capped GNPs (**b**) at different conditions.

DOX·HCl. This finding may be due to the replacement, shielding and masking of citrate anion on particle surface by the PEG chain. The higher zeta potential of GNPs capped with adsorbed DOX·HCl is due to the presence of ionized carboxyl group on the particle surface and also due to incomplete coverage of the carboxyl anions with DOX·HCl (33,46). (28,41). Additionally, the presence of the positively charged DOX HCl on particle surface was also believed to neutralize some of the surface negative charges due its extensive positive charge imparted by the drug's hydrochloride salt (44,47).

Effect of Sodium Chloride and Different pH Conditions on the Dispersion Stability of GNPs

The reduction of gold salts by sodium citrate produces nanoparticles with sufficient negative surface charges which is main reason for dispersion stability of citrate capped GNPs due to electrostatic repulsion (48). Thus, any agents that can mask or neutralize the surface negative charges of nanoparticles will result in dispersion instability and aggregation of nanoparticles. The aggregated nanoparticles are characterized by change of the color of nanoparticles solution from wine red to blue or violet, particle size increase observed with PCS and a shift of the maximum absorption peak (λ_{max}) to longer wave lengths. These additional absorption bands are caused by electric dipole-dipole interaction and coupling between plasmon of adjacent particles inside the aggregates and the decreased interparticle distances inside the aggregates (49).

Upon addition of the acetate buffer, PBS or sodium chloride to the merely citrate-stabilized GNPs, the color of colloidal gold solution gradually changed from red to blue followed by appearance of a new very broad absorption band in the UV-Vis spectrum above 550 nm (Fig. 3a) indicating the occurrence of aggregation (50,51). The very rapid aggregation of citrate-stabilized nanoparticles by the aforementioned reagents may be due to the shielding or neutralization of the surface negative charges and the subsequent reduction of the electrostatic repulsion between the individual particles (52,53). However, when acetate buffer, PBS buffer or NaCl were separately added to PEG-coated GNPs, the size and λ_{max} were not affected (Fig. 3b) because the surface PEGylated GNPs are mainly stabilized by steric stabilization of the attached hydrophilic polymers to their surfaces rather than electrostatic repulsion (8,46,54).

In order to characterize the particle aggregation, particle size of the non-PEGylated and PEGylated GNPs was measured in the different previously described conditions to help an understanding of the aggregation process. In addition, the apparent size mainly affects the biological applications of nanoparticles by destroying their biocompatibility (55,56). Figure 4a shows the effect of the addition of sodium chloride, PBS and acetate buffer on the size of GNPs, determined by photon correlation spectroscopy, of PEGylated and uncoated (citrate stabilized) particles.

It's obvious that sodium chloride had induced a large size increase of the citrate-stabilized GNPs most likely due to neutralization of most of negative surface charges of the particles. Unlikely, the effects of both PBS and acetate buffer on size of citrate-stabilized GNPs are smaller compared to that induced by sodium chloride which may be attributed to their lower ionic strength. Comparatively, the size of carboxy-PEG-AlkSH coated GNPs did not show marked size increase after sodium chloride, PBS or acetate buffer addition due their

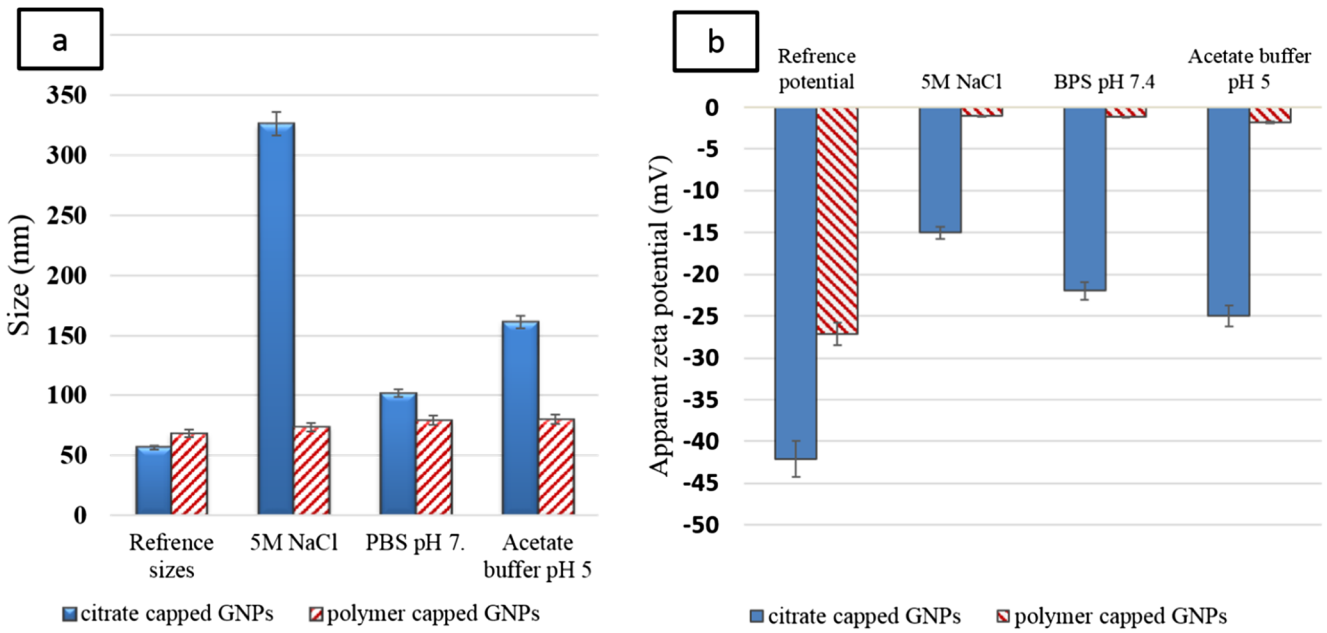

Fig. 4 Varied sizes of citrate and polymer capped GNPs in different ionic conditions (**a**) and the corresponding zeta potential (**b**).

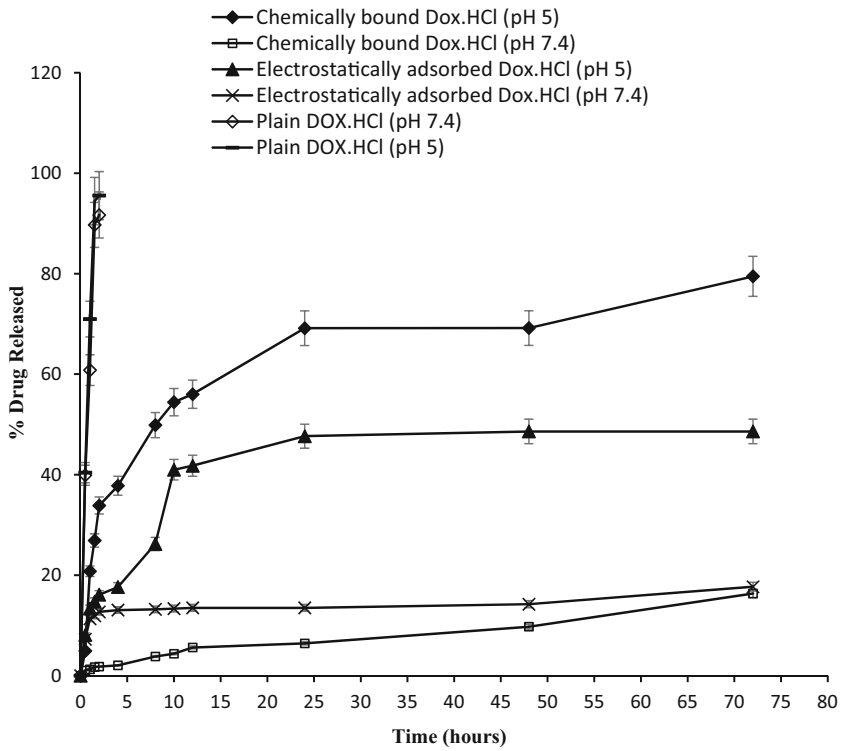

Fig. 5 *In-vitro* release profiles of plain and loaded DOX.HCl in both acetate (pH 5) buffer and PBS (pH 7.4).

stabilization by the polymer coating. These results confirm the previous UV-Vis spectroscopy findings however, similar results were reported in earlier studies (57,58).

The effects of sodium chloride, PBS and acetate buffer on the zeta potential of citrate-stabilized and carboxy-PEG coated GNPs are depicted in Fig. 4b. A pronounced increase of the zeta potential is observed for the citrate stabilized GNPs after addition of sodium chloride, PBS and acetate buffer which demonstrated the shielding and neutralization of most of the surface charges. The increase of the surface potential towards more positive values is observed after addition of the previous reagents to the carboxy-PEG-coated GNPs. This may be attributed to the adsorption of some sodium cations to the PEG chains or the formation of PEG-carboxylic acid salt.

In Vitro Release Study of the Prepared DOX·HCl Capped GNPs

The percent of DOX·HCl capped to the GNPs was estimated using eqs. 1 and 2. As shown in Table I, the drug capping capacity was found to be rather higher (99%) in case of the chemically bound DOX·HCl than the electrostatically adsorbed one (92%). The higher capping capacity of chemically bound drug compared to the adsorbed one could be due to the fact that, chemical binding of drug to polymer (covalent bonding) is stronger than the electrostatic attraction between the drug and polymer. The drug's release behaviors of both systems, compared to plain drug, in different pH values are illustrated in Fig. 5. The release of plain drug in both pH

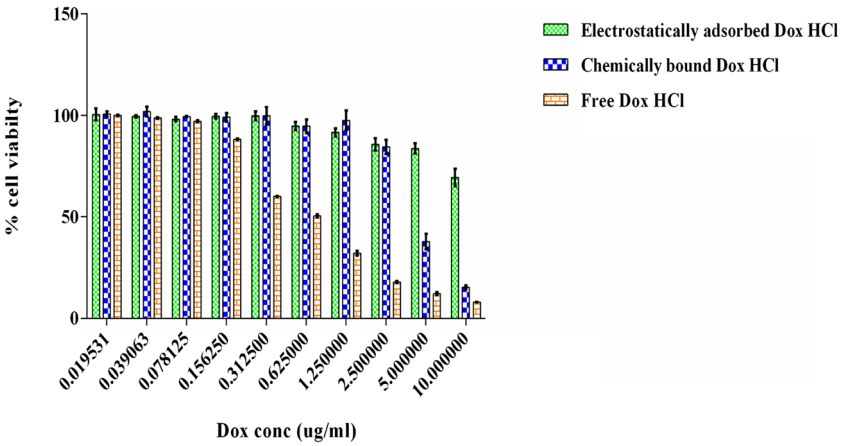

Fig. 6 Cell viability (%) of the electrostatically adsorbed DOX.HCl, chemically bound DOX.HCl and free DOX.HCl against human breast cancer cell line (MCF-7). Data is presented as mean ± SD.

Table II The IC_{50} Values for the Chemically and Electrostatically Bound Dox HCl Compared to Free Dox HCl

System	Free Dox HCl	Chemically bound Dox HCl	Electrostatically adsorbed Dox HCl
IC_{50} (ug/ml)	0.62	2.069	11.98

values (7.4 and 5) was almost completed during the first two hours of the release time. Other investigated systems, show a weak release behavior in the PBS (pH 7.4) where only (10%) of the chemically bound DOX·HCl was released while a larger amount (17.6%) of the electrostatically adsorbed DOX·HCl was released at this pH. These results may be attributed to the weak hydrolytic reaction of the hydrazone bond, at pH 7.4, (40,59) compared to the loose electrostatic attraction of the carboxy-PEG with DOX·HCl. In contrast, up to 80% of the chemically bound DOX·HCl was released in the acidic acetate buffer compared to about 50% drug release of the electrostatically adsorbed DOX·HCl following 72 h. Likely, these results are due to the higher hydrolytic impact of the acidic conditions on the pH sensitive hydrazone linker that led to this amount of DOX·HCl release (41,60). On the other hand, the electrostatically adsorbed DOX·HCl was not much influenced by the acidic environment due to the lack of the acid sensitive bond. This release behavior of DOX·HCl was in accordance with the previously reported result where 50% drug release was obtained following an external stimuli after 12 h (61). The release behavior obtained by developed systems, in comparison to the release behavior of plain drug, seems to be more advantageous as it is largely affected only by the pH conditions; without the use of any external stimulus with more sustained behavior that would last for several days. Moreover, the acid labile linker imparted by the hydrazone bond would be more beneficial as passive targeting strategy than the electrostatic adsorption strategy due to the smaller amount of drug leakage in normal physiological environment (pH 7.4) and the higher release activity in cancerous tissues where the slightly acidic condition is available. Eventually, both systems may be helpful in reducing the systematic adverse effects and toxicity caused by premature release of loaded drug during circulation in the blood.

In Vitro Cell Viability Assay of Doxorubicin Capped GNPs against MCF-7 Breast Cancer Cell Line

The cytotoxic activity of the developed systems was evaluated against human breast adenocarcinoma (MCF-7) cells using MTT assay where the obtained viability results were compared to free DOX·HCl as positive control. Reportedly, uncoated GNPs possess no cytotoxicity towards MCF-7 cells and hence the developed cytotoxicity results were only attributed to the loaded DOX·HCl (62).

As shown in Fig. 6, at the higher DOX·HCl concentration (10 μg/ml), the maximum count percent for viable cells were 15.4% and 65.4% for the chemically bound and the electrostatically adsorbed DOX.HCl respectively. Compared to the cytotoxic effect of free DOX·HCl (8.2%), it is obvious that, the chemically bound DOX·HCl has the greater cytotoxicity profile than the electrostatically adsorbed one. However, the cytotoxic activity decreased with the reduction of the amount of DOX·HCl in all groups.

The calculated IC_{50} values, as shown in Table II, proved that the cytotoxic effects of free DOX·HCl and the chemically bound DOX·HCl were much higher than the cytotoxic effect of the electrostatically adsorbed DOX·HCl. Furthermore, the obtained results were compared using the non-parametric "kruskall-wallis" test as depicted in Table III. It was found that there was no statistical significance between free DOX·HCl and the chemically bound DOX HCl at p‡0.05, which indicated the higher cytotoxicity of the chemically designed GNPs system. Also, there were higher statistical significances between the electrostatically bound DOX·HCl and the other compared groups at P‡0.05 which implies for a lower cytotoxic effect of the electrostatically bound DOX·HCl than the free or the chemically bound DOX·HCl. However, this enhanced cytotoxicity may be attributed to the effect of chemical binding by the hydrazone linker on drug release.

CONCLUSIONS

Based on PEGylated GNPs, a comparative study was held to understand the influence of the well-known acid sensitive hydrazone linker and its rule in the passive-targeted delivery of DOX·HCl to cancerous tissues. The covalent linking strategy was compared to a non-covalent adsorption one and it was found that the hydrazone linking strategy has shown a marked acid sensitivity than the electrostatic adsorption which was proven by the previously discussed release behavior in the

Table III Non-Parametric ANOVA "Kruskall-Wallis" Test Results Showing the *p* Values for the Cytotoxicity Profiles of the Compared Systems

Compared systems	Electrostatically Adsorbed *vs* chemically bound Dox HCl	chemically bound *vs* free Dox HCl	Electrostatically adsorbed *vs* free Dox HCl
P value	0.045*	0.45	0.041*

*P‹0.5

acidic environment. Moreover, the hydrazone linked drug showed slower release rate in the normal physiological pH conditions compared to the electrostatically adsorbed drug which is highly recommended feature for the reduction of premature drug release. The cytotoxicity results against MCF-7 cancer cells confirmed that the acid sensitive covalent linking of DOX·HCl was more effective in reduction of growth of cancer than the electrostatically adsorbed one. Additionally, statistical analysis of the cytotoxicity results showed significant differences in favor of both free and chemically bound DOX·HCl on the expense of the electrostatically bound DOX·HCl. In conclusion, the covalent binding of DOX·HCl to nanomaterials via pH sensitive linkers could be beneficial and promising as a passive targeting strategy than the non-covalent binding. This new approach would help improve efficacy and reduce the side effects of such cytotoxic drugs.

REFERENCES

1. Clarke R, Leonessa F, Multidrug TB. Resistance/P-glycoprotein and breast Cancer: Review and meta-analysis. Semin Oncol. 2005;32(Supplement 7):9–15.
2. Wang J, Wu L, Kou L, Xu M, Sun J, Wang Y, et al. Novel nanostructured enoxaparin sodium-PLGA hybrid carriers overcome tumor multidrug resistance of doxorubicin hydrochloride. Int J Pharm. 2016;513(1):218–26.
3. Brigger I, Dubernet C, Couvreur P. Nanoparticles in cancer therapy and diagnosis. Adv Drug Deliv Rev. 2002;54(5):631–51.
4. Connor EE, Mwamuka J, Gole A, Murphy CJ, Wyatt MD. Gold nanoparticles are taken up by human cells but do not cause acute cytotoxicity. Small. 2005;1(3):325–7.
5. Ruan S, Yuan M, Zhang L, Hu G, Chen J, Cun X, et al. Tumor microenvironment sensitive doxorubicin delivery and release to glioma using angiopep-2 decorated gold nanoparticles. Biomaterials. 2015;37:425–35.
6. Choi SH, Byeon HJ, Choi JS, Thao L, Kim I, Lee ES, et al. Inhalable self-assembled albumin nanoparticles for treating drug-resistant lung cancer. J Control Release. 2015;197:199–207.
7. Zhang G, Yang Z, Lu W, Zhang R, Huang Q, Tian M, et al. Influence of anchoring ligands and particle size on the colloidal stability and in vivo biodistribution of polyethylene glycol-coated gold nanoparticles in tumor-xenografted mice. Biomaterials. 2009;30(10):1928–36.
8. Gao J, Huang X, Liu H, Zan F, Ren J. Colloidal stability of gold nanoparticles modified with thiol compounds: Bioconjugation and application in Cancer cell imaging. Langmuir. 2012;28(9):4464–71.
9. Liu X, Huang N, Wang H, Li H, Jin Q, Ji J. The effect of ligand composition on the in vivo fate of multidentate poly(ethylene glycol) modified gold nanoparticles. Biomaterials. 2013;34(33):8370–81.
10. Bednarski M, Dudek M, Knutelska J, Nowiński L, Sapa J, Zygmunt M, et al. The influence of the route of administration of gold nanoparticles on their tissue distribution and basic biochemical parameters: in vivo studies. Pharmacol Rep. 2015;67(3):405–9.
11. Carvalho C, Santos RX, Cardoso S, Correia S, Oliveira PJ, Santos MS, et al. Doxorubicin: the good, the bad and the ugly effect. Curr Med Chem. 2009;16(25):3267–85.
12. Thorn CF, Oshiro C, Marsh S, Hernandez-Boussard T, McLeod H, Klein TE, et al. Doxorubicin pathways: pharmacodynamics and adverse effects. Pharmacogenet Genomics. 2011;21(7):440–6.
13. Wilczewska AZ, Niemirowicz K, Markiewicz KH, Car H. Nanoparticles as drug delivery systems. Pharmacol Rep. 2012;64(5):1020–37.
14. del Rosario LS, Demirdirek B, Harmon A, Orban D, Uhrich KE. Micellar Nanocarriers assembled from doxorubicin-conjugated amphiphilic macromolecules (DOX–AM). Macromol Biosci. 2010;10(4):415–23.
15. Guerzoni LPB, Nicolas V, Angelova A. In vitro modulation of TrkB receptor signaling upon sequential delivery of curcumin-DHA loaded carriers towards promoting neuronal survival. Pharm Res. 2017;34(2):492–505.
16. Angelova A, Garamus VM, Angelov B, Tian Z, Li Y, Zou A. Advances in structural design of lipid-based nanoparticle carriers for delivery of macromolecular drugs, phytochemicals and anti-tumor agents. Adv Colloid Interf Sci. 2017;249:331–45.
17. Angelova A, Angelov B, Drechsler M, Lesieur S. Neurotrophin delivery using nanotechnology. Drug Discov Today. 2013;18(23):1263–71.
18. Chen Y, Angelova A, Angelov B, Drechsler M, Garamus VM, Willumeit-Romer R, et al. Sterically stabilized spongosomes for multidrug delivery of anticancer nanomedicines. J Mater Chem B. 2015;3(39):7734–44.
19. Zerkoune L, Lesieur S, Putaux J-L, Choisnard L, Geze A, Wouessidjewe D, et al. Mesoporous self-assembled nanoparticles of biotransesterified cyclodextrins and nonlamellar lipids as carriers of water-insoluble substances. Soft Matter. 2016;12(36):7539–50.
20. Paciotti GF, Myer L, Weinreich D, Goia D, Pavel N, McLaughlin RE, et al. Colloidal gold: a novel nanoparticle vector for tumor directed drug delivery. Drug Delivery. 2004;11(3):169–83.
21. El-Sayed IH, Huang X, El-Sayed MA. Selective laser photothermal therapy of epithelial carcinoma using anti-EGFR antibody conjugated gold nanoparticles. Cancer Lett. 2006;239(1):129–35.
22. Turkevich J, Stevenson PC, Hillier J. A study of the nucleation and growth processes in the synthesis of colloidal gold. Discuss Faraday Soc. 1951;11(0):55–75.
23. Che E, Wan L, Zhang Y, Zhao Q, Han X, Li J, et al. Development of phosphonate-terminated magnetic mesoporous silica nanoparticles for pH-controlled release of doxorubicin and improved tumor accumulation. Asian J Pharm Sci. 2014;9(6):317–23.
24. Mahou R, Wandrey C. Versatile route to synthesize heterobifunctional poly (ethylene glycol) of variable functionality for subsequent pegylation. Polymers. 2012;4(1):561–89.
25. Shenoy D, Fu W, Li J, Crasto C, Jones G, DiMarzio C, et al. Surface functionalization of gold nanoparticles using hetero-bifunctional poly (ethylene glycol) spacer for intracellular tracking and delivery. Int J Nanomedicine. 2006;1(1):51–8.
26. Woghiren C, Sharma B, Stein S. Protected thiol-polyethylene glycol: a new activated polymer for reversible protein modification. Bioconjug Chem. 1993;4(5):314–8.
27. Napoli A, Tirelli N, Kilcher G, Hubbell A. New synthetic methodologies for amphiphilic multiblock copolymers of ethylene glycol and propylene sulfide. Macromolecules. 2001;34(26):8913–7.
28. Volcker N, Klee D, Hanna M, Hocker H, Bou JJ, Ilarduya Ad, *et al.* Synthesis of heterotelechelic poly (ethylene glycol) s and their characterization by MALDI-TOF-MS. Macromol Chem Phys 1999;200(6):1363–1373.
29. Bogdanov AA. Graft-copolymer stabilized metal nanoparticles. US patent. 2015;
30. Moldt T, Brete D, Przyrembel D, Das S, Goldman JR, Kundu PK, et al. Tailoring the properties of surface-immobilized Azobenzenes by monolayer dilution and surface curvature. Langmuir. 2015;31(3):1048–57.

31. Overberger C, O'shaughnessy M, Shalit H. The preparation of some aliphatic azo nitriles and their decomposition in solution. J Am Chem Soc. 1949;71(8):2661–6.
32. Herrwerth S, Rosendahl T, Feng C, Fick J, Eck W, Himmelhaus M, et al. Covalent coupling of antibodies to self-assembled monolayers of Carboxy-functionalized poly(ethylene glycol): protein resistance and specific binding of biomolecules. Langmuir. 2003;19(5):1880–7.
33. Zayed G, Tessmar JK. Heterobifunctional poly (ethylene glycol) derivatives for the surface modification of gold nanoparticles toward bone mineral targeting. Macromol Biosci. 2012;12(8): 1124–36.
34. Prime KL, Whitesides GM. Adsorption of proteins onto surfaces containing end-attached oligo(ethylene oxide): a model system using self-assembled monolayers. J Am Chem Soc. 1993;115(23): 10714–21.
35. Li JJ. Williamson ether synthesis. Name Reactions: Springer; 2014. p. 628-.
36. Witt D, Klajn R, Barski P, Grzybowski BA. Applications, properties and synthesis of -functionalized n-Alkanethiols and disulfides - the building blocks of self-assembled monolayers. Curr Org Chem. 2004;8(18):1763–97.
37. Nudelman A, Bechor Y, Falb E, Fischer B, Wexler BA, Nudelman A. Acetyl chloride-methanol as a convenient reagent for: A) quantitative formation of amine hydrochlorides B) carboxylate Ester formation C) mild removal of N-t-Boc-protective group. Synth Commun. 1998;28(3):471–474.
38. Ellman GL. Tissue sulfhydryl groups. Arch Biochem Biophys. 1959;82(1):70–7.
39. Tyuftin AA, Solovieva SE, Murav'ev AA, Polyantsev FM, Latypov SK, Antipina IS. Thiacalix[4] arenes with terminal thiol groups at the lower rim: synthesis and structure. Russ Chem Bull. 2009;58(1): 145–51.
40. Patil R, Portilla-Arias J, Ding H, Konda B, Rekechenetskiy A, Inoue S, et al. Cellular delivery of doxorubicin via pH-controlled hydrazone linkage using multifunctional nano vehicle based on poly (β-L-malic acid). Int J Mol Sci. 2012;13(9):11681–93.
41. Wang F, Wang Y-C, Dou S, Xiong M-H, Sun T-M, Wang J. Doxorubicin-tethered responsive gold nanoparticles facilitate intracellular drug delivery for overcoming multidrug resistance in Cancer cells. ACS Nano. 2011;5(5):3679–92.
42. Etrych T, Mrkvan T, Chytil P, Koňák Č, Říhová B, Ulbrich K. N-(2-hydroxypropyl)methacrylamide-based polymer conjugates with pH-controlled activation of doxorubicin. I. New synthesis, physicochemical characterization and preliminary biological evaluation. J Appl Polym Sci. 2008;109(5):3050–61.
43. Frens G. Controlled nucleation for the regulation of the particle size in monodisperse gold suspensions. Nature. 1973;241(105):20–2.
44. Madhusudhan A, Reddy GB, Venkatesham M, Veerabhadram G, Kumar DA, Natarajan S, et al. Efficient pH dependent drug delivery to target cancer cells by gold nanoparticles capped with carboxymethyl chitosan. Int J Mol Sci. 2014;15(5):8216–34.
45. Gu Y-J, Cheng J, Man CW-Y, Wong W-T, Cheng SH. Gold-doxorubicin nanoconjugates for overcoming multidrug resistance. Nanomedicine. 2012;8(2):204–11.
46. Corbierre MK, Cameron NS, Lennox RB. Polymer-stabilized gold nanoparticles with high grafting densities. Langmuir. 2004;20(7): 2867–73.
47. Vigevani A, Doxorubicin WMJ. Doxorubicin. In: Klaus F, editor. Analytical profiles of drug substances. Volume 9: academic press; 1981. p. 245–74.
48. Norman TJ, Grant CD, Magana D, Zhang JZ, Liu J, Cao D, et al. Near infrared optical absorption of gold nanoparticle aggregates. J Phys Chem B. 2002;106(28):7005–12.
49. Chah S, Hammond MR, Zare RN. Gold nanoparticles as a colorimetric sensor for protein conformational changes. Chem Biol. 12(3):323–8.
50. Burns C, Spendel WU, Puckett S, Pacey GE. Solution ionic strength effect on gold nanoparticle solution color transition. Talanta. 2006;69(4):873–6.
51. Nam J, Won N, Jin H, Chung H, Kim S. pH-induced aggregation of gold nanoparticles for Photothermal Cancer therapy. J Am Chem Soc. 2009;131(38):13639–45.
52. Aryal S, RB KC, Bhattarai N, Kim CK, Kim HY. Study of electrolyte induced aggregation of gold nanoparticles capped by amino acids. J Colloid Interface Sci. 2006;299(1):191–7.
53. Wang G, Sun W. Optical limiting of gold nanoparticle aggregates induced by electrolytes. J Phys Chem B. 2006;110(42):20901–5.
54. Takae S, Akiyama Y, Otsuka H, Nakamura T, Nagasaki Y, Kataoka K. Ligand density effect on Biorecognition by PEGylated gold nanoparticles: regulated interaction of RCA120 lectin with lactose installed to the distal end of tethered PEG strands on gold surface. Biomacromolecules. 2005;6(2):818–24.
55. Jo DH, Kim JH, Lee TG, Kim JH. Size, surface charge, and shape determine therapeutic effects of nanoparticles on brain and retinal diseases. Nanomedicine. 2015;11(7):1603–11.
56. Chavanpatil MD, Khdair A, Patil Y, Handa H, Mao G, Panyam J. Polymer-surfactant nanoparticles for sustained release of water-soluble drugs. J Pharm Sci. 2007;96(12):3379–89.
57. Zayed G, Tessmar J, Gopferich A. Development of colloids for cell and tissue targeting: bisphosphonate-functionalized gold nanoparticles for the investigation of bone targeting. In: phD; 2010.
58. Miyamoto D, Oishi M, Kojima K, Yoshimoto K, Nagasaki Y. Completely dispersible PEGylated gold nanoparticles under physiological conditions: modification of gold nanoparticles with precisely controlled PEG-b-polyamine. Langmuir. 2008;24(9):5010–7.
59. Lu D, Wen X, Liang J, Gu Z, Zhang X, Fan Y. A pH-sensitive nano drug delivery system derived from pullulan/doxorubicin conjugate. J Biomed Mater Res B Appl Biomater. 2009;89B(1):177–83.
60. Sun T-M, Wang Y-C, Wang F, Du J-Z, Mao C-Q, Sun C-Y, et al. Cancer stem cell therapy using doxorubicin conjugated to gold nanoparticles via hydrazone bonds. Biomaterials. 2014;35(2):836–45.
61. Zhang Z, Wang L, Wang J, Jiang X, Li X, Hu Z, et al. Mesoporous silica-coated gold Nanorods as a light-mediated multifunctional Theranostic platform for Cancer treatment. Adv Mater. 2012;24(11):1418–23.
62. François A, Laroche A, Pinaud N, Salmon L, Ruiz J, Robert J, et al. Encapsulation of docetaxel into PEGylated gold nanoparticles for vectorization to Cancer cells. ChemMedChem. 2011;6(11): 2003–8.